

Picosecond energy relaxation rates of hot excitonic molecules in CdSe

A. S. Vengurlekar, S. S. Prabhu, and S. K. Roy

Tata Institute of Fundamental Research, Bombay 400005, India

J. Shah

AT & T Bell Laboratories, Holmdel, New Jersey 07733

(Received 7 June 1994)

We measure the time- and energy-resolved luminescence due to hot biexcitons in CdSe at 8 K using picosecond upconversion spectroscopy. The biexciton luminescence rises with a time constant of 12 ps following picosecond photoexcitation of electrons and holes. It then decays with a time constant of 240 ps. The time dependent luminescence spectrum is used to deduce the hot biexciton energy relaxation rates in CdSe. We compare the results with theoretical calculations based on phonon emission by biexcitons.

In a highly excited semiconductor, a large number of free electron-hole (e - h) pairs are generated. The carriers relax to their respective band edges by fast emission of optical phonons, whenever possible energetically, and by slower emission of acoustic phonons. Also the e - h pairs can form excitons. If the excitation density is large enough, the excitons may interact with each other to form excitonic molecules (biexcitons).^{1,2} Results of several theoretical studies and numerical calculations have shown³ that such a bound state of two excitons is possible in many semiconductors. The biexcitons can get annihilated in a spontaneous radiative decay into a photon polariton, leaving behind an exciton polariton. The experimental evidence for biexcitons has been obtained in giant two photon absorption experiments⁴ and by observing the characteristic biexciton luminescence and its excitation intensity dependence in semiconductors such as CuCl (Ref. 5) and CdS.⁶ Recently, biexcitons in GaAs quantum wells have been studied⁷ using two-photon absorption and self-diffraction techniques. Assuming parabolic excitonic and biexcitonic energy bands, the energy-momentum conservation in the biexciton radiative decay, ignoring the photon momentum, leads to the equation, $h\nu = E_x^0 - E_{bM} - \hbar^2 k_M^2 / 4m_x$, where $h\nu$ is the energy of the emitted photon, $E_x^0 = E_g - E_{bx}$ is the exciton ground state energy, E_g is the band gap energy, E_{bx} and E_{bM} , respectively, are exciton and biexciton binding energies, \vec{k}_M is the biexciton momentum wave vector, and m_x is the exciton effective mass. The biexcitons undergo elastic collisions among themselves and with excitons. They also interact with phonons. Under the action of these processes, the biexcitons may attain quasithermal equilibrium among themselves. The relaxation time related to the biexciton-biexciton collisions, which partly determines the formation time of a thermal, hot biexciton energy distribution, can be estimated, using a simple geometric argument² to be of the order of 1 ps in CdSe. Assuming that the biexcitons have a thermalized energy distribution, given by $f_M(\epsilon_M) = C \exp(-\epsilon_M / kT_M)$, $\epsilon_M = \hbar^2 k_M^2 / 4m_x$, T_M is the biexciton effective temperature ($\geq T_L$, the lattice temperature) and by comparing the observed lumines-

cence spectrum with a theoretical expression based on this, the biexciton effective temperatures have been determined in the past in the case of CdS (Ref. 6) and CuCl (Ref. 8) under steady illumination conditions. By creating a biexciton assembly using a picosecond laser pulse excitation and obtaining the time-resolved biexciton luminescence energy spectrum, it should be possible to determine the hot biexciton cooling behavior and, thereby, the biexciton energy relaxation rates. To our knowledge, this information is not available so far in spite of much work devoted to the study of biexciton properties. In this paper, we report the first measurements of hot biexciton cooling rates in CdSe and compare the experimental results with a theoretical calculation based on biexciton interactions with optical phonons via the Fröhlich mechanism, and with acoustic phonons via the deformation potential and piezoelectric couplings in CdSe.

In our experiments, we excite CdSe crystals at 8 K using a pulsed Nd YAG (yttrium aluminum garnet) pumped rhodamine 6G dye laser, with an autocorrelation pulse width of 1.8 ps. The time-resolved measurements are made using the upconversion luminescence spectroscopy in a standard photon counting setup. The time resolution is 2.5 ps and the energy resolution is about 2.5 meV in these measurements. The average beam intensity is varied from 1 mW to 10 mW to obtain an average e - h pair excitation density per pulse (n_0) estimated to be in the range $n_0 = 8 \times 10^{16} - 8 \times 10^{17} \text{ cm}^{-3}$. (A possible underestimate of the laser spot size on the sample by 10 μm will reduce the density estimate by 30%.) The well known luminescence features related to the bound exciton (I_2) and the biexciton in CdSe (Ref. 9) can be identified and separated by using intensity dependent measurements of time-integrated (TI) and photoexcitation-correlation (PEC) luminescence spectra.^{10,11} Figure 1 shows that while the low intensity TI and PEC measurements show signals mainly due to the bound exciton at 1.823 eV, the biexciton related luminescence is clearly evident at about 1.821 eV at higher intensities. This identification of emission due to I_2 and the biexciton is in good agreement with the previous luminescence measurements in CdSe.^{9,11} We obtain the time-resolved luminescence spectrum in the

energy region covering the bound exciton and biexciton emission, at various delays (up to a maximum of 1 ns) and excitation densities of $n_0 = 8 \times 10^{16}$, 4×10^{17} , and $8 \times 10^{17} \text{ cm}^{-3}$. This is illustrated in the examples of Fig. 2 in which we show the luminescence energy spectrum taken at different delays for $n_0 = 8 \times 10^{17} \text{ cm}^{-3}$. It is interesting to note that the luminescence signal first appears just as the free carriers are generated by the exciting pulse (width of 1.8 ps). This suggests that the excitons and biexcitons can form even before the free e - h pairs fully relax. On the other hand, the luminescence may be due to the combined effect of e - h plasma (with renormalized band gap) and biexcitons in the early stages.

Within a simple perturbation theory, the biexciton emission spectrum is given by²

$$I(\nu) = \frac{2\pi}{\hbar} \sum_{\vec{k}_M} |M_{bx \rightarrow x}|^2 f_M(\epsilon_M) \times \delta[h\nu - E_x(\vec{k}_M) - E_M(\vec{k}_M)], \quad (1)$$

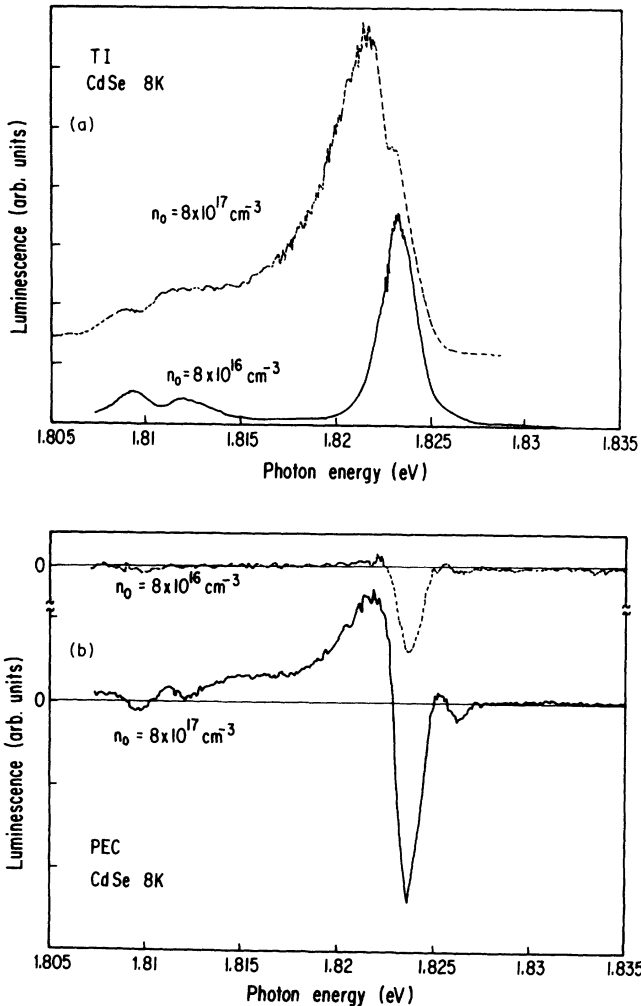


FIG. 1. The time-integrated (a) and photoexcitation-correlation (at 100 ps) (b) luminescence energy spectra are shown for low ($n_0 = 8 \times 10^{16} \text{ cm}^{-3}$) and high ($n_0 = 8 \times 10^{17} \text{ cm}^{-3}$) density excitations.

where $M_{bx \rightarrow x}$ is the matrix element for biexciton \rightarrow exciton radiative decay, $f_M(\epsilon_M)$ is the biexciton energy distribution, and $E_x(\vec{k}_M)$ and $E_M(\vec{k}_M)$ are, respectively, exciton and biexciton energies at \vec{k}_M . Equation (1) does not include the effects of biexciton-biexciton and biexciton-exciton elastic collisions. These are not very important at sufficiently low excitation densities. Assuming that the matrix element in Eq. (1) for the biexciton radiative decay is independent of \vec{k}_M and that the biexcitons have a thermalized energy distribution, we have, at low densities,²

$$I(\nu) = A' \sqrt{\epsilon_M} \exp(-\epsilon_M/kT_M), \quad (2)$$

where $\epsilon_M = \hbar^2 k_M^2 / 4m_x = E_x^0 - E_{bM} - h\nu$. At high excitation densities, a more appropriate description of the biexciton emission spectrum is obtained by including the biexciton collision effects and is given by^{4,6}

$$I(\nu) = A \int \frac{\Gamma \sqrt{\epsilon'} \exp(-\epsilon'/kT_M) d\epsilon'}{[(\epsilon_M - \epsilon')^2 + \Gamma^2]}, \quad (3)$$

where Γ^{-1} refers to the sum of relaxation times of biexciton and exciton momentum states. [Eq. (3) reduces to Eq. (2) when $\Gamma/kT \ll 1$.] Since the bound exciton energy in CdSe is higher than the biexciton ground state energy by only 1 meV or so,^{6,12} a line shape analysis of the complete spectra is not simple. The emission spectra on the high energy side of the peaks in Fig. 2 may have some effects of the bound exciton recombination in addition to those of the collision broadened biexciton emission spectrum. This may be relatively more important for low excitation densities and long delays than for higher densities and smaller delays at which the biexcitons dominate and the bound excitons are saturated. On the other hand, the spectra on the lower energy side of the bound exciton are predominantly due to the biexciton decay. We compare this part of the spectra ($h\nu < 1.823 \text{ eV}$) with Eq. (3), treating Γ , $E_x^0 - E_{bM}$ and T_M as parameters. The agreement of the low energy side of the spectra with the behavior predicted within the above model of hot biexciton emission spectra [Eq. (3)] is excellent, as shown in Fig. 2. The literature values of E_{bM} are quoted to be 4 meV (Ref. 6) to 5 meV.¹² We have used $E_{bM} = 4.5 \text{ meV}$ in these calculations. Figure 2 (inset) also shows the total (energy integrated) biexciton luminescence as a function of time. The biexciton luminescence rises with a time constant of 12 ps. The signal reaches its peak in about 30 ps and then has an exponential decay with a time constant of 240 ps. These time constants have been obtained for CdSe for the first time. We note, however, that determination of the biexciton formation and decay rates requires analysis of the coupled dynamics of free and bound excitons, biexcitons, and free carriers not attempted here. The value of Γ obtained from the fit in Fig. 2 depends on the excitation density and is time dependent, as shown in Fig. 3 (inset). The rather large value of r required to fit the data for small delays is probably due to our having ignored the e - h plasma effects. The biexciton effective temperature T_M obtained at various delays and excitation densities is shown in Fig. 3. It turns out that the peak position of the

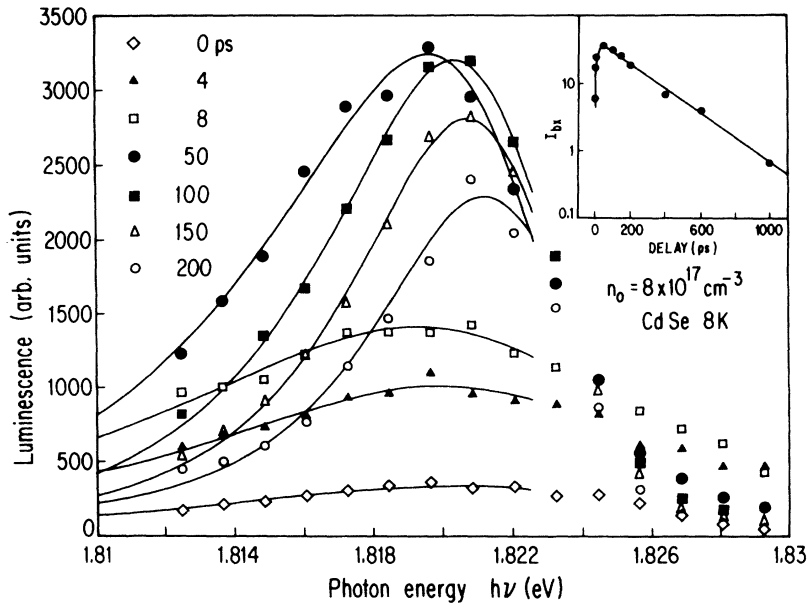


FIG. 2. The time-resolved luminescence energy spectra shown at various delays at $8 \times 10^{17} \text{ cm}^{-3}$ together with theoretical fits (continuous curves) based on Eq. (3). The inset shows the total (integrated) biexciton luminescence I_{bx} as a function of time.

spectra measured at the lowest excitation density used in our experiments ($n_0 = 8 \times 10^{16} \text{ cm}^{-3}$) shifts from 1.82 eV at generation to the energy expected for the bound exciton (1.823 eV) beyond 200 ps. This implies that although the low energy tail of the luminescence spectra is due to biexcitons, the luminescence at 1.823 eV for long delays evolves into that predominantly due to bound exciton radiative recombination for $n_0 = 8 \times 10^{16} \text{ cm}^{-3}$. An attempt to fit the data in this case using Eq. (3) leads to values of Γ larger than those obtained for much higher

excitation densities (Fig. 3, inset). Since Γ is expected to decrease as the excitation density decreases, we conclude that Eq. (2) rather than Eq. (3) adequately describes the data at $n_0 = 8 \times 10^{16} \text{ cm}^{-3}$. The cooling behavior appears to be independent of the excitation density within the experimental errors ($\sim 10\text{--}20\%$).

The biexciton cooling rate is determined by the energy loss rates due to phonon emission via various biexciton-phonon couplings. Writing $3kdT_M/dt = -\langle d\epsilon_M/dt \rangle$, k being the Boltzmann constant, we can determine $\langle d\epsilon_M/dt \rangle$, the average energy loss rate per biexciton in CdSe, using the data (and the dashed curve drawn to fit the data) of Fig. 3. The energy loss rate thus obtained is shown in Fig. 4 (continuous curve).

For a comparison with the energy loss rates expected theoretically, we note that the average energy loss rate

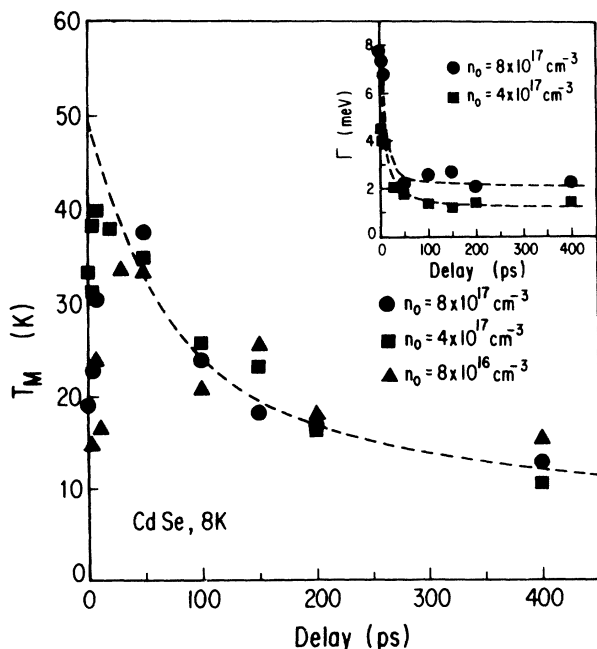


FIG. 3. The biexciton effective temperature (T_M) shown at various delays and excitation densities. The dashed curve is drawn to guide the eye. The inset shows Γ (Γ is the sum of biexciton and exciton collision induced relaxation frequencies,^{4,6} see text).

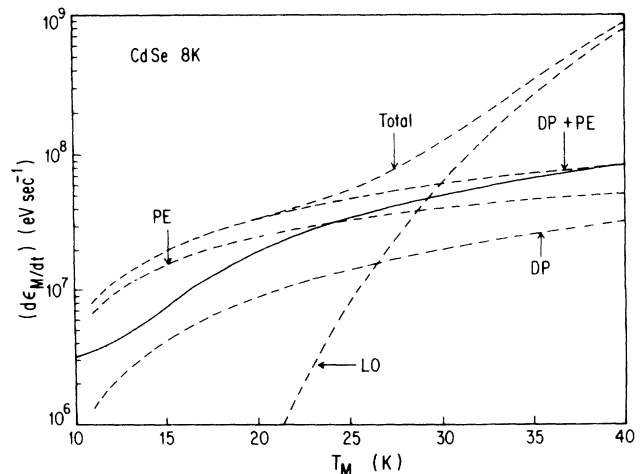


FIG. 4. The experimental (continuous curve) biexciton energy relaxation rate (for $n_0 = 8 \times 10^{17} \text{ cm}^{-3}$) is compared with theory (dashed curves) based on phonon emission by biexcitons.

due to phonon emission is given by¹³

$$\langle d\epsilon_M/dt \rangle = \sum_s \frac{1}{n_M 2\pi^2} \int_0^\infty \hbar\omega_q^s q^2 \left(\frac{\partial N_q^s}{\partial t} \right) dq, \quad (4)$$

where s denotes the phonon coupling mechanism, n_M is the biexciton density, V is the crystal volume, N_q^s and $\hbar\omega_q^s$, respectively, are the occupancy and energy of phonons of type s . For optical phonons, $\hbar\omega_q^s \simeq \hbar\omega_0$ and for acoustic phonons $\hbar\omega_q^s \simeq \hbar uq$, where u is the sound velocity and q is the phonon wave vector. Assuming a Maxwell-Boltzmann biexciton energy distribution, the phonon generation rate $\partial N_q^s/\partial t$ is given by¹⁴

$$\frac{\partial N_q^s}{\partial t} = n_M V \frac{(2\pi)^{1/2}}{(\hbar)^2} \sqrt{m_M/kT_M} \frac{|M_q^s|^2}{q} e^{-(\epsilon_{\min}^s + X_q^s)}, \quad (5)$$

where m_M is the biexciton effective mass (equal to $2m_x$), $X_q = \hbar\omega_q^s/kT_M$, $\epsilon_{\min}^s = (\hbar^2/8m_M kT_M) \times [q - (2m_M \hbar\omega_q^s/\hbar^2 q)]^2$, and M_q^s is the matrix element describing the biexciton-phonon interactions. The biexciton-phonon couplings have not been calculated so far, but may be written in analogy with those for exciton-phonon interactions.^{4,15} Thus we have, for the Fröhlich coupling of biexciton with longitudinal optical (LO) phonons,

$$|M_q^{\text{LO}}(q)| = \frac{1}{q} (q_e - q_h) \sqrt{\frac{2\pi \hbar\omega_{\text{LO}} e^2}{V} \left(\frac{1}{\epsilon_\infty} - \frac{1}{\epsilon_0} \right)}, \quad (6)$$

$$q_{e(h)} = \{1 + [(qa_x/2)m_{e(h)}/m_x]^2\}^{-2}, \quad (7)$$

a_x is the exciton Bohr radius, $m_{e(h)}$ is the electron (hole) effective mass, $\hbar\omega_{\text{LO}}$ is the LO phonon energy, and $\epsilon_\infty(0)$ is the optical (static) dielectric constant. For deformation potential (DP) and piezoelectric (PE) acoustic phonon

coupling, we have, respectively,

$$|M_q^{\text{DP}}(q)| = (\hbar/2\rho uV)^{1/2} q^{1/2} (D_c q_e - D_v q_h), \quad (8)$$

$$|M_q^{\text{PE}}(q)| = (\hbar/2\rho uV)^{1/2} [4\pi e \hat{e}_{\text{pe}}/\epsilon_0 q^{1/2}] (q_e - q_h), \quad (9)$$

where ρ is the crystal mass density, $D_{c(v)}$ the deformation potential for the conduction (valence) band, and \hat{e}_{pe} the effective piezoelectric coupling constant. Using Eqs. (2)–(6), we can calculate $\langle d\epsilon_M/dt \rangle$ for various values of T_M . For such a calculation, we use the following CdSe parameters:^{15,16} $m_e = 0.13m_0$, $m_h = 0.8m_0$, m_0 is the rest mass of the electron, $\epsilon_0 = 9.75$, $\epsilon_\infty = 6.75$, $\rho = 5.81$ gms/cm³, $\hbar\omega_{\text{LO}} = 26.5$ meV, $a_x = 5.36$ nm, $u = 2.391 \times 10^5$ cm/sec, $D_c = 4.2$ eV, $D_v = 2.2$ eV, $\hat{e}_{\text{pe}} = 0.0144$ (0.0189) C²/m⁴ for the longitudinal (transverse) acoustic phonon case. Since the biexciton-phonon coupling parameters are yet to be determined, but may be similar to the exciton-phonon case, we have assumed here that the known exciton-phonon coupling parameters¹⁵ are also valid for the biexciton case. The calculated energy loss rates (dashed curves) are shown in Fig. 4 together with the experimental rate (for $n_0 = 8 \times 10^{17}$ cm⁻³) deduced from the data of Fig. 3. The theory based on Eqs. (3)–(8) is seen to give a total energy loss rate somewhat larger than that obtained experimentally. This suggests that the biexciton-phonon couplings may be weaker than those for exciton-phonon interactions. It should be interesting to investigate this aspect in more detail.

In conclusion, we have made time- and energy-resolved measurements of the biexciton luminescence spectrum in CdSe at 8 K. Using these, we have deduced the hot biexciton energy relaxation rates in CdSe.

This work was partly supported by the NSF under Grant Nos. INT-9022623 and INT-9201350.

¹M. A. Lampert, Phys. Rev. Lett. **1**, 450 (1958); S. A. Moskalenko, J. Opt. Spectrosc. **5**, 147 (1958).

²E. Hanamura and H. Haug, Phys. Rep. **33**, 4 (1977).

³J. M. Levi-Lelond, Phys. Rev. **178**, 1526 (1969); O. Akimoto and E. Hanamura, J. Phys. Soc. Jpn. **33**, 1537 (1972); W. F. Brinkman, T. M. Rice, and B. Bell, Phys. Rev. B **8**, 1570 (1973).

⁴M. Ueta, H. Kanzaki, K. Kobayashi, Y. Toyozawa, and E. Hanamura, *Excitonic Processes in Solids* (Springer-Verlag, Berlin 1986).

⁵S. Nikitine, in *Excitons at High Density*, edited by H. Haken and S. Nikitine (Springer-Verlag, Berlin, 1975).

⁶S. Shionoya, H. Saito, E. Hanamura, and O. Akimoto, Solid State Commun. **12**, 223 (1973).

⁷D. J. Lovering, R. T. Phillips, G. J. Denton, and G. W. Smith, Phys. Rev. Lett. **68**, 1880 (1992).

⁸N. Nagasawa, N. Nakata, Y. Doi, and M. Ueta, J. Phys. Soc. Jpn. **38**, 593 (1975); **39**, 987 (1975).

⁹M. Hayashi, H. Saito, and S. Shionoya, J. Phys. Soc. Jpn. **44**, 582 (1978).

¹⁰D. Rosen, A. G. Doukas, Y. Budansky, K. Katz, and R. R. Alfano, Appl. Phys. Lett. **39**, 935 (1981).

¹¹M. Jorgensen and J. M. Hvam, Appl. Phys. Lett. **43**, 460 (1983).

¹²J. M. Hvam, I. Balslev, and B. Honerlage, Europhys. Lett. **4**, 839 (1987).

¹³E. M. Conwell, *High Field Transport in Semiconductors*, edited by F. Seitz, D. Turnbull, and H. Ehrenreich, Solid State Physics Suppl. 9 (Academic, New York, 1967).

¹⁴S. M. Kogan, Fiz. Tverd. Tela (Leningrad) **4**, 2474 (1963) [Sov. Phys. Solid State **4**, 1813 (1963)].

¹⁵Y. Masumoto and S. Shionoya, Phys. Rev. B **30**, 1076 (1984).

¹⁶*Data in Science and Technology*, edited by O. Madelung, Landolt-Börnstein, New Series, Group III, Vol. 17, Pt. b (Springer-Verlag, Heidelberg, 1982).